Detection of HF Toward PKS 1830-211, Search for Interstellar H2F+, and Laboratory Study of H2F+ and H2Cl+ Dissociative Recombination

The Astrophysical Journal, 822:115 (9pp), 2016 May 10 doi:10.3847/0004-637X/822/2/115

DETECTION OF HF TOWARD PKS 1830–211, SEARCH FOR INTERSTELLAR H_2F^+, AND LABORATORY STUDY OF H_2F^+ AND H_2Cl^+ DISSOCIATIVE RECOMBINATION

K. Kawaguchi[1], S. Muller[2], J. H. Black[2], T. Amano[3], F. Matsushima[4], R. Fujimori[5], Y. Okabayahsi[1], H. Nagahiro[1], Y. Miyamoto[1], and J. Tang[1]

[1] Graduate School of Natural Science and Technology, Okayama University, Okayama 700-8530, Japan
[2] Department of Earth and Space Sciences, Chalmers University of Technology, Onsala Space Observatory, SE-43992 Onsala, Sweden
[3] Department of Chemistry and Department of Physics and Astronomy, University of Waterloo, Waterloo, ON, N2L 3G1, Canada
[4] Department of Physics, Faculty of Science, University of Toyama, Toyama 930-8555, Japan
[5] Institute for Space-Earth Environmental Research, Nagoya University, Nagoya 464-8601, Japan
Received 2016 January 5; accepted 2016 March 13; published 2016 May 12

ABSTRACT

We report extragalactic observations of two fluorine-bearing species, hydrogen fluoride (HF) and fluoronium (H_2F^+), in the $z = 0.89$ absorber in front of the lensed blazar PKS 1830−211 with the Atacama Large Millimeter/submillimeter Array. HF was detected toward both southwest and northeast images of the blazar, with column densities $>3.4 \times 10^{14}$ cm^{-2} and 0.18×10^{14} cm^{-2}, respectively. H_2F^+ was not detected, down to an upper limit (3σ) of 8.8×10^{11} cm^{-2} and an abundance ratio of $[H_2F^+]/[HF] \leqslant 1/386$. We also searched for H_2F^+ toward the Galactic sources NGC 6334 I and W51C, and toward Galactic center clouds with the *Herschel* HIFI spectrometer.[6] The upper limit on the column density was derived to be 2.5×10^{11} cm^{-2} in NGC 6334 I, which is 1/68 of that for H_2Cl^+. In constrast, the ortho transition of H_2Cl^+ is detected toward PKS 1830–211. To understand the small abundance of interstellar H_2F^+, we carried out laboratory experiments to determine the rate constants for the ion–electron recombination reaction by infrared time-resolved spectroscopy. The constants determined are $k_e(209\ \mathrm{K}) = (1.1 \pm 0.3) \times 10^{-7}$ cm^3 s^{-1} and $(0.46 \pm 0.05) \times 10^{-7}$ cm^3 s^{-1} for H_2F^+ and H_2Cl^+, respectively. The difference in the dissociative recombination rates between H_2F^+ and H_2Cl^+ by a factor ∼2 and the cosmic abundance ratio $[F]/[Cl] \approx 1/6$ are not enough to explain the much smaller abundance of H_2F^+. The difference in the formation mechanism of H_2F^+ and H_2Cl^+ in interstellar space would be a major factor in the small abundance of H_2F^+.

Key words: galaxies: individual (PKS 1830–211) – ISM: individual objects (W31C, NGC 6334 I) – ISM: molecules – methods: laboratory: molecular

1. INTRODUCTION

The hydrogen fluoride (HF) molecule was first detected in space by Neufeld et al. (1997) toward Sgr B2, using the *Infrared Space Observatory*. Later, CF^+ was detected toward the Orion bar region (Neufeld et al. 2006), where the detection was driven by a theoretical study (Neufeld et al. 2005) of fluorine-bearing molecules in the interstellar medium. HF and CF^+ are significant fluorine-bearing molecules in interstellar space, while AlF was detected in a circumstellar envelope by Cernicharo & Guélin (1987). Recently, HF was detected in many interstellar clouds with the Heterodyne Instrument for the Far-Infrared (HIFI) on board the *Herschel* Space Observatory (Neufeld et al. 2010; Phillips et al. 2010; Sonnentrucker et al. 2010, 2015; Monje et al. 2011a). HF was also detected in four nearby galaxies: in Mrk 231 (van der Werf et al. 2010, in emission) and Arp 220 (Rangwala et al. 2011) with the *Herschel* SPIRE-FTS, and in NGC 253 and NGC 4945 using HIFI (Monje et al. 2014). The detection of HF toward a high-redshift quasar at $z = 2.56$ was reported by Monje et al. (2011b) using the Caltech Submillimeter Observatory. The observed abundance of HF in diffuse clouds was found to be consistent with theoretical predictions of Neufeld et al. (2005), Neufeld & Wolfire (2009), and Sonnentrucker et al. (2015), where in the latest report they carried out some updates of reaction data and also included grain surface chemistry.

In the present paper, we report the detection of HF in the $z = 0.89$ molecular absorber toward PKS 1830−211 and searches for H_2F^+ toward PKS 1830−211 and other Galactic sources. H_2F^+ is isovalent with H_2Cl^+ and isoelectronic to H_2O. In 2010, Lis et al. reported the detection of H_2Cl^+ toward NGC 6334 I and Sgr B2 with HIFI. Recently, H_2Cl^+ was also detected toward PKS 1830−211 (Muller et al. 2014a) with the Atacama Large Millimeter/submillimeter Array (ALMA). The existence of the related H_2F^+ ion in interstellar clouds would be interesting from the viewpoint of halogen chemistry. A purely rotational spectroscopic study of H_2F^+ was reported by Fujimori et al. (2011), who measured five rotational lines of H_2F^+ in the ground state by using a submillimeter-wave spectrometer based on a backward-wave oscillator (BWO) at the University of Waterloo. Since the BWO measurement was limited in the frequency region below 775 GHz, higher frequency transitions were covered by a tunable far-infrared spectrometer at the University of Toyama (Amano et al. 2012), and seven lines were detected in the region 1305–1851 GHz. These spectroscopic studies made it possible to search for H_2F^+ in interstellar space. However, the rotational transition frequencies from the lowest state are not accessible to ground-based telescopes because of atmospheric absorption. Therefore, observations were carried out toward the $z = 0.89$ molecular-rich absorber in front of PKS 1830−211 (see, e.g., Muller et al. 2011) using the ALMA and toward Galactic sources with the *Herschel* Space Observatory.

The *Herschel* Space Observatory detected many new interstellar molecules and molecular ions. In particular, H_2O^+ (Ossenkopf et al. 2010), HCl^+ (De Luca et al. 2012),

[6] *Herschel* is an ESA space observatory with science instruments provided by European-led Principal Investigator consortia and with important participation from NASA.

H_2Cl^+ (Lis et al. 2010), and ArH^+ (Schilke et al. 2014) were first detected in relatively low-density clouds with H_2 density of less than $10^3\,cm^{-3}$. The proton affinity of HF (484 kJ mol^{-1}) is larger than that of H_2 (422 kJ mol^{-1}), but smaller than those of CO (594 kJ mol^{-1}) and N_2 (494 kJ mol^{-1}). Therefore, low-density clouds become potentially good candidates for searching for H_2F^+. Since H_2F^+ has been thought to be produced through the reaction of H_3^+ and HF, H_2F^+ may be a direct proxy for H_3^+ in diffuse clouds.

In spite of sensitive searches for H_2F^+ in the present study, the ion is still not detected in space. Its abundance depends on production and/or depletion mechanisms. In diffuse clouds, the depletion is dominated by dissociative recombination reactions with electrons. Neufeld et al. (2005) and Neufeld & Wolfire (2009) estimated the rate constant k_e for the following dessociative recombination reactions in their chemical study of fluorine-bearing molecules:

$$H_2F^+ + e \rightarrow HF + H \quad k_e = 3.5 \times 10^{-7}(T/300\,K)^{-0.5}\,cm^3\,s^{-1} \quad (1)$$

$$H_2F^+ + e \rightarrow F + products \quad k_e = 3.5 \times 10^{-7}(T/300\,K)^{-0.5}\,cm^3\,s^{-1}. \quad (2)$$

Various kinds of experimental methods have been reported for determining the recombination rate constants, as summarized by Plašil et al. (2002) and Geppert & Larsson (2008). Adam & Smith (1988) reported $k_e = 1 \times 10^{-7}\,cm^3\,s^{-1}$ at 300 K for $H_2F^+ + e$ by a flowing afterglow/Langmuir probe method. This value is seven times smaller than the value calculated from Equations (1) and (2) at 300 K. Nowadays storage ring experiments are well applied for measurements of dissociative recombination rate constants, such as those of H_3^+ (McCall et al. 2004) and HCl^+ (Novotny et al. 2013). The method has an advantage in measurement of the temperature dependence of the reaction rate. Neufeld et al. (2012) assumed the following k_e value of H_2Cl^+, where storage ring data were cited as a private communication:

$$H_2Cl^+ + e \rightarrow Cl + products \quad k_e = 1.2 \times 10^{-7}(T/300\,K)^{-0.85}cm^3\,s^{-1}. \quad (3)$$

At 50 K (approximately the kinetic temperature of low-density clouds), Equations (1) and (2) give $k_e = 1.7 \times 10^{-6}\,cm^3\,s^{-1}$ for H_2F^+, and Equation (3) gives $k_e = 5.5 \times 10^{-7}\,cm^3\,s^{-1}$ for H_2Cl^+, which is about 1/3 of that of H_2F^+. To check the difference in the recombination rate constants, the present paper reports measurements of the rate constants for the reactions of H_2F^+ and H_2Cl^+ ions with electrons by using an infrared OPO (optical parametric oscillator) laser coupled with a time-resolved method. Previously, the method of time-resolved infrared laser absorption has been applied to determine the rate constants of H_3^+, HCO^+, and HN_2^+ by Amano (1988, 1990). Later it was found that the determined k_e value for H_3^+ is close to the value obtained by storage ring experiments (McCall et al. 2004).

2. ASTRONOMICAL OBSERVATIONS

2.1. ALMA Observations

We obtained ALMA Cycle 2 observations of the H_2F^+ 1_{10}–1_{01} transition (rest frequency of 760.929 GHz, redshifted to 403.5 GHz, i.e., in ALMA band 8) and HF $J = 1$–0 transition (rest frequency of 1232.4762 GHz, redshifted to 653.5 GHz, i.e., in ALMA band 9) on 2015 May 14 and May 19, respectively. We adopt a redshift of $z_{abs} = 0.88582$, heliocentric frame, giving $v = 0\,km\,s^{-1}$ for the absorption toward the SW image of PKS 1830−211.

The ALMA correlator was configured with four different spectral windows of 1.875 GHz, each counting 960 channels separated by 1.938 MHz, providing velocity resolutions of ~1.4 and 0.9 km s^{-1} after Hanning smoothing, in bands 8 and 9, respectively. The spectral windows were centered at ~401.5, 403.5, 413.8, and 415.5 GHz in band 8, and ~648.0, 649.9, 651.7, and 653.6 GHz in band 9. In band 8, we also observed the ortho-H_2Cl^+ 2_{12}–1_{01} line (rest frequency of 781.6 GHz). No other lines were detected in the frequency coverage of band 9.

The data calibration was done within the CASA[7] package, following a standard procedure. The bandpass response of the antennas was calibrated from observations of the bright quasar J1924−292. The complex gain solutions were determined by self-calibration of the visibilities of PKS 1830−211, using a simple model of two point sources at the positions of the two lensed images of the blazar. Using a Clean deconvolution (with Briggs weighting and robust parameter set to 0.5), we obtained synthesized beams of $0\farcs39 \times 0\farcs29$ (position angle PA = −84°) in band 8 and $0\farcs21 \times 0\farcs19$ (PA = 64°) in band 9. The two lensed images of PKS 1830−211, separated by ~1″, were spatially well resolved. The spectra were extracted toward both images using the CASA-python task UVMULTIFIT (Martí-Vidal et al. 2014) to fit a model of two point sources to the visibilities.

2.2. Herschel Observations

On 2013 February 26–March 7, the H_2F^+ ion was searched for toward four sources, W31C (star-forming region, α_{2000}: 18° 10′28.″70, β_{2000}: −19°55′50.″00), NGC 6334 I (high-mass star-forming region, α_{2000}: 17°20′53.″32, β_{2000}: −35°46′58.″5), GC IRS 21 (α_{2000}: 17°45′40.″20, β_{2000}: −29°0′31.″00), and 2Mass J17470898-2829561 (J1747) (α_{2000}: 17°47′8.″980, β_{2000}: −28° 29′56.″10), where the former two sources are known to have abundant HF and H_2Cl^+. In the latter two sources near the Galactic center, the H_3^+ ion has been detected strongly by infrared observations (Goto et al. 2008, 2011). We searched for two transitions, $J_{KaKc} = 2_{12}$–1_{01} (1850.082 GHz) and 1_{10}–1_{01} (760.929 GHz), from the lowest energy state of ortho levels. We used the dual-beam switch mode and the wideband spectrometer of the *Herschel*/HIFI spectrograph with a spectral resolution of 1.1 MHz ($\Delta v = 0.43\,km\,s^{-1}$ at 760 GHz). The observed data of level 2 were provided as calibrated DSB spectra. The integration time was 8 minutes for each source in the 761 GHz region, and 34 minutes for W31C, 43 minutes for NGC 6334 I, 33 minutes for GC IRS 21, and 31 minutes for 2 Mass J1747 in the 1850 GHz region. The frequency region of the 1_{11}–0_{00} line from the para ground state was not covered by *Herschel*/HIFI because of a lack of the detector system in the

[7] http://casa.nrao.edu/

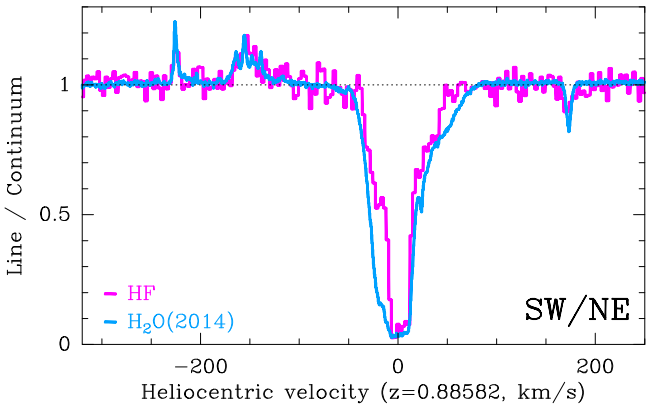

Figure 1. Spectrum of the HF $J = 1$–0 line. Data were smoothed to a velocity resolution of 2.8 km s^{-1}. The normalized spectrum toward the SW image has been divided by that toward the NE image in order to remove small bandpass residuals. The SW and NE absorptions appear as features <1 and >1, respectively. The normalized spectrum of the ground-state transition of ortho-H_2O 1_{10}–1_{01}, observed in 2014 July, is shown for comparison. The velocity scale is referenced to the heliocentric frame taking $z = 0.88582$.

region. The HF $J = 1$–0 transition at 1232.47 GHz was also observed toward NGC 6334 I and two sources near the Galactic center with an integration time of 7 minutes.

3. LABORATORY EXPERIMENTS FOR DISSOCIATIVE RECOMBINATIONS OF H_2F^+ AND H_2Cl^+

A continuous-wave OPO laser with a spectral width of about 0.8 MHz was used to cover the 3 μm infrared region in the present experiment (Okabayashi et al. 2015). It has a bow-tie-type cavity, and a PPLN crystal is pumped by a fiber laser (iPG Photonics YAR-25 K-LP-SF), which is seeded by a DFB laser (Koheras Y10-PM). The output of the OPO laser in the 3 μm region was 70 mW for a pumping power of the fiber laser of 6–8 W. The H_2F^+ ion was produced by a pulsed hollow-cathode discharge in a mixture of 5% F_2/He and H_2 gas with partial pressures of 70 mTorr (9.3 Pa) and 330 mTorr (44 Pa), respectively. A high-voltage transistor switch HTS 81 (Behlke Electronic GmbH) was used for the pulsed discharge with peak current of 200 mA. In the case of H_2Cl^+, a mixture of HCl and H_2 was used with partial pressures of 50 mTorr (6.6 Pa) and 330 mTorr (44 Pa). The same absorption measurement system was used as in a previous Fourier-transform infrared (FTIR) study of H_2F^+ (Fujimori et al. 2013) to attain an effective path length of 40 m with a multipath cell arrangement. The glass part of the cell had an inner diameter of 94 mm and a length of 1 m for the hollow-cathode discharge, and was connected to two glass tubes of inner diameter 144 mm and length of 250 mm on both sides, keeping a mirror separation of 150 cm. The cathode was made of a stainless plate of thickness 0.1 mm and mounted on the inner part of the glass cell. The discharge part was cooled by dry-ice. The transmitted laser beam was detected by an infrared mercury–cadmium–telluride detector (Vigo PVI-3TE-4, time constant of 20 ns) followed by a preamplifier (MIPDC-F-100, bandwidth of DC–100 MHz).

4. RESULTS

4.1. ALMA Observations of the z = 0.89 Absorber Toward PKS 1830−211

Figure 1 shows the observed absorption due to the HF $J = 1$–0 transition toward PKS 1830−211. Toward the southwest (SW) image, the absorption spans a velocity range between about −50 and +50 km s^{-1} and is heavily saturated near $v = 0$ km s^{-1}. Toward the northeast (NE) image, the absorption covers a velocity range between about −250 and −100 km s^{-1} and reaches at most ∼20% of the continuum level. For comparison, we also show in Figure 1 the absorption spectrum of the ground-state transition of ortho-water, obtained in 2014 April with ALMA. The profiles are nearly identical along the NE line of sight, but the HF absorption has narrower wings than H_2O toward the SW image. Note, however, that time variations of the absorption profiles, with a timescale of months to years, have been observed in this absorber (Muller & Guélin 2008; Muller et al. 2014b) and somewhat limit the direct comparison of spectra taken at different epochs.

Assuming that all HF molecules are in the ground state of $J = 0$, the column density is obtained by using the following formula:

$$N_{\rm HF} = \frac{8\pi^{3/2} \times \Delta v}{2\sqrt{\ln 2} \times \lambda^3 \times A} \frac{g_l}{g_u} \times \tau \quad (4)$$

where λ is the wavelength (243.2 μm), A the Einstein A-coefficient (2.422×10^{-2} s^{-1}), and g_l and g_u are the statistical weights of the lower and upper states. τ is the optical depth and is given by

$$\tau = -\ln\left(\frac{T_{\rm MB}}{T_{\rm back}}\right), \quad (5)$$

where $T_{\rm MB}$ and $T_{\rm back}$ are the measured brightness temperature and the background continuum temperature, respectively. In the SW direction, by using the linewidth of 20 km s^{-1}, the lower limit of τ is estimated to be 4 from a simulation of the shape of the absorption line. On the other hand, the τ value of NE is obtained to be 0.21. The column densities are determined to be

$$N_{\rm HF}({\rm SW}) > 3.4 \times 10^{14}\ {\rm cm}^{-2} \quad [{\rm HF}]/[{\rm H_2}] > 1.7 \times 10^{-8}$$
$$N_{\rm HF}({\rm NE}) = 0.18 \times 10^{14}\ {\rm cm}^{-2} \quad [{\rm HF}]/[{\rm H_2}] = 1.8 \times 10^{-8}$$

where the abundance relative to H_2 is calculated by assuming an H_2 column density of $\sim 2 \times 10^{22}$ cm^{-2} in SW and $\sim 1 \times 10^{21}$ cm^{-2} in NE (Muller et al. 2014b). In the Milky Way, the relative abundance of HF is reported to be 2.5×10^{-8} in NGC 6334 I and 1.5×10^{-8} in AFGL 2591 (Emprechtinger et al. 2012), 0.8×10^{-8} in IRC+10216 (Agúndez et al. 2011), $(1.1–1.6) \times 10^{-8}$ in W51 and W49N (Sonnentrucker et al. 2010), a conservative lower limit of 0.6×10^{-8} in W31C (Neufeld et al. 2010), and 1.6×10^{-10} in the Orion hot core (Phillips et al. 2010). Sonnentrucker et al. (2015) estimated the HF abundance in Galactic diffuse clouds by using a modified chemical reaction model and found $[{\rm HF}]/[{\rm H_2}] = (0.9–3.3) \times 10^{-8}$, which is consistent with the observed values including those of 12 newly observed sources. The currently obtained abundance in the $z = 0.89$ absorber is thus close to the values of low-density Galactic clouds.

The redshifted 403 GHz region for the H_2F^+ 1_{10}–1_{01} transition was observed, as shown in Figure 2. The absorption due to H_2F^+ is not found, and the rms noise level (1σ) is estimated to be 0.5% with 4.2 km s^{-1} channels. The absorption occurs from the lowest rotational level of the ortho H_2F^+ level, and the second lowest level 1_{10} is located at an energy 37 K

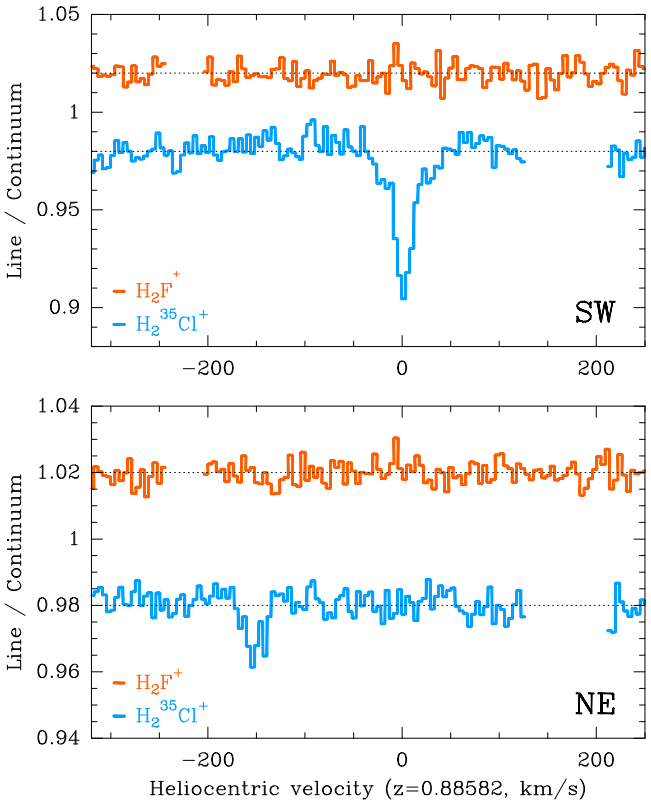

Figure 2. Spectra of the H_2F^+ 1_{10}–1_{01} and H_2Cl^+ 2_{12}–1_{01} lines, toward the SW image (top) and NE image (bottom), observed simultaneously in the same tuning. Data were smoothed to a velocity resolution of 4.2 km s^{-1}. Regions with atmospheric lines were flagged. The velocity scale is referenced to the heliocentric frame taking $z = 0.88582$.

higher than the 1_{01} level. Since the H_2 density of the absorbing gas is relatively low (a few 10^3 cm^{-3}), the excitation of polar species is coupled to the photons of the cosmic microwave background (CMB), with $T_{CMB} = 5.14$ K at $z = 0.89$ (see Muller et al. 2013). We assume that all ortho state molecules are present in the lowest 1_{01} state. By using Equations (4) and (5), we derive the upper limit (3σ) for the ortho state of the ion to be

$$N_{H2F+}(SW) = 6.6 \times 10^{11}\,cm^{-2}$$

where the A-coefficient is 0.0200 s^{-1} and λ is 394 μm for the 1_{10}–1_{01} transition, and we assumed a velocity width of 20 km s^{-1}. Table 1 lists the upper limit for the total abundance, including the para state population by assuming an ortho-to-para ratio of 3. It is known that some molecules with ortho-to-para ratios smaller than 3 have been detected, and such molecules are thought to be produced on the surface of low-temperature dust or grains. Some molecules produced by ion–molecule reactions in the gas phase have ratios smaller than 3 (Takakuwa et al. 2001; Morisawa et al. 2006; Faure et al. 2013), originating from abundant para-H_2 in cold clouds. However, in the case of H_2Cl^+, ratios very different from 3 have not been reported (Neufeld et al. 2015), so the assumption of the high-temperature limit value may be valid for H_2Cl^+ and also H_2F^+. It is found that the abundance of H_2F^+ is less than 1/386 of that of HF.

In the same line of sight, Muller et al. (2014a) reported a column density of H_2Cl^+ of $\sim 1.4 \times 10^{13}$ cm^{-2} from the observation of the para transition 1_{11}–0_{00} and by assuming an ortho-to-para ratio of 3. In the present observation, the ortho transition 2_{12}–1_{01} was detected, as shown in Figure 2. The integrated intensity (opacity) has been obtained as 2.03 km s^{-1} and 0.71 km s^{-1} toward SW and NE, respectively, and the column density of the ortho ions is estimated to be 9.1×10^{12} cm^{-2} and 3.2×10^{12} cm^{-2} by assuming that all ortho ions are in the lowest rotational 1_{01} level. The ortho-to-para ratio is 2.7 and 3 in SW and NE, respectively, which are consistent with the high-temperature limit value. Time variations of the absorption profiles (Muller & Guélin 2008) might affect this measurement of the ortho-to-para ratio for H_2Cl^+. Observations close in time would allow us to obtain a very robust ortho-to-para ratio in the two independent lines of sight. The H_2F^+ abundance is found to be less than 1/16 of that of H_2Cl^+.

Table 1
Abundances of H_2F^+, H_2Cl^+, HF, HCl, and H_2 (Column Density (cm^{-2}))

Species	PKS 1830−211[a]	W31C	NGC 6334 I
H_2F^+	$\lesssim 8.8 \times 10^{11}$	$\lesssim 8.1 \times 10^{11}$	$\lesssim 2.5 \times 10^{11}$
H_2Cl^+	$\sim 1.4 \times 10^{13}$[b]	3.0×10^{13}[c]	1.7×10^{13}[d]
HF	$>3.4 \times 10^{14}$	1.6×10^{14}[e]	$(0.4–2.4) \times 10^{13}$[f]
HCl	3.4×10^{13}[g]	$\sim 2 \times 10^{13}$[h]	1.9×10^{14}[i]
H_2	$\sim 2 \times 10^{22}$[j]	1.2×10^{22}[k]	$(0.6\text{-}1.8) \times 10^{21}$[f]

Notes.
[a] SW line of sight.
[b] Muller et al. (2014a).
[c] Neufeld et al. (2012).
[d] Lis et al. (2010).
[e] Neufeld et al. (2010).
[f] In the foreground components (Emprechtinger et al. 2012).
[g] S. Muller et al. (2016, in preparation).
[h] Monje et al. (2013).
[i] $T_{ex} = 39$ K component (Zernickel et al. 2012).
[j] Muller et al. (2011).
[k] H_1 abundance (Godard et al. 2010).

4.2. Herschel *Observations of Galactic Clouds: Search for Interstellar H_2F^+*

The HF $J = 1$–0 spectral line was detected toward NGC 6334 I with many saturated absorption components, as reported by Emprechtinger et al. (2012). Spectra observed toward W31C and NGC 6334 I in the 760 GHz region are shown in Figure 3. In the two Galactic center sources GC IRS 21 and 2Mass J1747, no emission and absorption lines have been detected, where the background continuum level was 0.1 K and 0.03 K, respectively. The low continuum levels compared with 3σ noise levels of 0.1 K in both objects make it difficult to detect absorption lines. Many emission lines have been detected in W31C and NGC 6334 I, and assignments and analyses of these spectral lines will be reported in a separate paper. The H_2F^+ line is expected to be observed as absorption, because the ion is thought to be present in low-density clouds as H_2Cl^+, which is observed as absorption. Toward W31C and NGC 6334 I there was no feature of an absorption line in the 760 GHz region, as shown in Figure 3. In the 1850 GHz region, the noise level was 10–18 times larger than that in the 760 GHz region, so the sensitivity was not enough to detect the H_2F^+ line. We estimated the upper limit for the column density to be 1.9×10^{11} cm^{-2} in the ortho state toward NGC 6334 I, where we used three times (0.080 K) the rms noise and assumed a

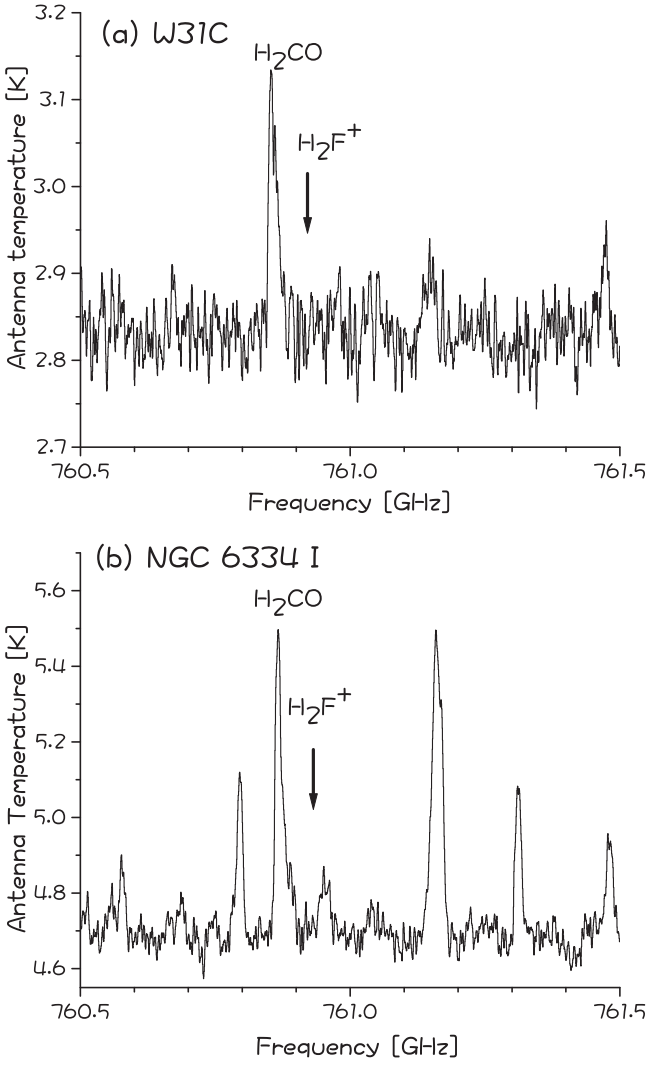

Figure 3. Search for the H_2F^+ 1_{10}–1_{01} spectral line toward W31C and NGC 6334 I, where the frequency scale is given by using the systemic velocities of -3 km s^{-1} and -1.7 km s^{-1}, respectively. The H_2CO line ($J_{KaKc} = 10_{19}$–9_{18}) is observed in the lower side band at 749.0721 GHz.

velocity width of 4.93 km s^{-1}. Similarly, the upper limit toward W31C was estimated by using $3\sigma = 0.090$ K and assuming a width of 9.5 km s^{-1}. The width corresponds to one velocity component among three or four components in the foreground gas of W31C. Table 1 lists total abundances, including the para state population of H_2F^+ and related species. Since the abundance of H_2Cl^+ has been reported to be 1.7×10^{13} cm^{-2} (Lis et al. 2010), which is 4.3% of that of HCl (4×10^{14} cm^{-2}) in NGC 6334 I, the abundance of H_2F^+ is found to be 1/68 of that of H_2Cl^+. The solar abundance ratio of F and Cl is reported to be 804/5170 ~ 1/6 (Lodders et al. 2009) in the solar photosphere, although an old value of 1/2 is quoted in our previous paper (Fujimori et al. 2011). The small abundance of H_2F^+ compared with the cosmic atomic abundance may be explained by differences in production and/or depletion mechanisms.

4.3. Laboratory Time-resolved Infrared Laser Spectroscopy of H_2F^+ and H_2Cl^+

Figure 4 shows the observed time-resolved spectrum of the $H_2F^+\nu_3$ band, $J_{KaKc} = 3_{13} \leftarrow 4_{14}$ transition at 3251.99 cm^{-1} (Fujimori et al. 2013). We also measured the time profile for the $H_2Cl^+\nu_3$, $J_{KaKc} = 6_{06} \leftarrow 5_{05}$ and $6_{16} \leftarrow 5_{15}$ transitions at 2691.24 cm^{-1} (Lee et al. 1988), as shown in Figure 5. The time profile shows a rise in absorption due to the ion at the beginning of the pulsed discharge, and after turning off the discharge the absorption intensity of the ion signal decreases with a half-life of a few tens of microseconds. The rotational relaxation time of the ground state is expected to be less than 1 μs, when we assume a pressure-broadening coefficient of 10–20 MHz Torr^{-1}. Therefore, the observed decay is thought to be due to the recombination reaction with an electron. There are many species in the discharge in addition to the reactant F_2, He, and H_2 species. If a product species with a larger proton affinity than HF is present, the proton of H_2F^+ moves to the species, and the decay of H_2F^+ will be affected compared with the case of just the recombination reaction with an electron. However, the proton transfer occurs at the Langevin rate ($\sim 10^{-9}$ cm^{-3} s^{-1}), which is two orders of magnitude smaller than the rate of the recombination reaction. Among reactants and products in the discharge, F, F_2, He, H, and H_2 have smaller proton affinities than HF. On the other hand, HF dimer and trimer are thought to have larger proton affinities than HF. However, the spectra of these species were not observed by FTIR (Fujimori et al. 2013) in the same discharge condition, indicating much smaller abundances than HF. So the effects of proton transfer reactions will be neglected in the analysis of the decay of H_2F^+.

In a reaction $N^+ + e^- \rightarrow$ products, the time variation of the ion density is expressed as follows:

$$-\frac{d[N^+]}{dt} = k_e[N^+][e^-]. \quad (6)$$

When the density of positive ions is equal to that of electrons, the following relation is attained (the second-order reaction scheme):

$$\frac{1}{[N^+(t)]} = k_e \times t + \frac{1}{[N^+(0)]}. \quad (7)$$

In the case of H_3^+, Amano (1988) could explain the observed decay by Equation (7). On the other hand, the observed decay of H_2F^+ of Figure 4(a) was not fitted to the formula of Equation (7) as shown in Figure 4(b), and the decay was found to be fitted to an exponential function as shown in Figure 4(c). This indicates that the reaction proceeds in the pseudo-first-order scheme. That is, by assuming $[e^-] \gg [N^+(t)]$,

$$\ln[N^+(t)] = -k_e[e^-]t + \ln[N^+(0)] \quad (8)$$

where $[N^+(0)]$ is the abundance at the starting time of decay $t = 0$. For H_2Cl^+, the same exponential fitting as H_2F^+ was found to be better. In the first-order reaction scheme, the electron density is higher than that of H_2F^+ or H_2Cl^+. For neutrality of the discharge plasma producing H_2F^+, other positive ions should carry the positive charge. Although positive ions such as F_2^+, F^+, H^+, He^+, and protonated $(HF)_2$ will be candidates, we did not monitor these species in the present experiment. In a pure hydrogen discharge, the H_3^+ ion was observed by FTIR (Fujimori et al. 2013), but the spectrum disappeared when the F_2/He gas mixture was added to the discharge. In the present discharge, the H_2F^+ ion is thought to be produced by reactions $H_2^+ + HF$ and $HF^+ + H_2$, where we monitored the HF absorption with FTIR. The HF^+ ion was observed by laser

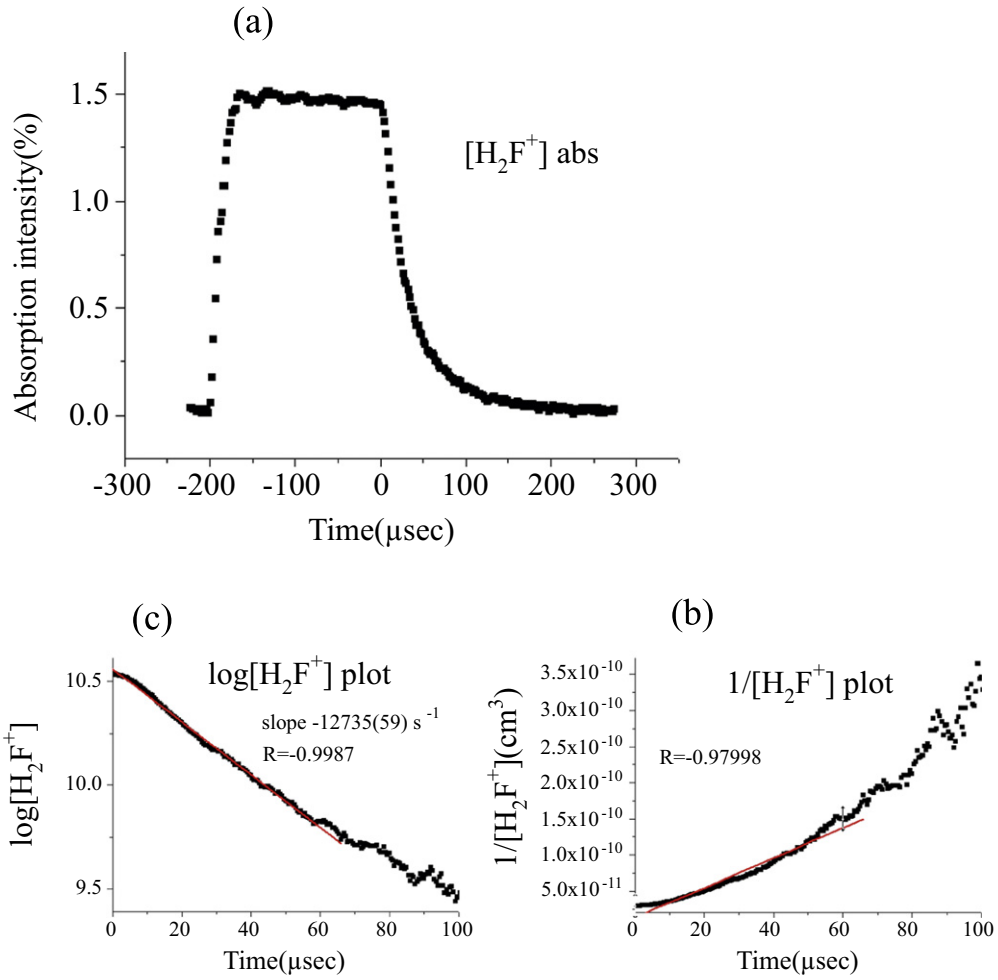

Figure 4. (a) Time-resolved spectrum of the $H_2F^+\nu_3$ band, $J_{KaKc} = 3_{13} \leftarrow 4_{14}$ transition at 3251.99 cm^{-1} obtained by a pulsed discharge with peak current of 200 mA, (b) $1/N$ fit, (c) exponential fit.

spectroscopy (Hovde et al. 1989) in a discharge of a mixture of a large amount of He and HF. In the present condition, the ion was not observed with FTIR in the 3.3 μm region, because of rapid reaction with H_2.

By least-squares fittings of the observed decay curves, we determined the $k_e[e^-]$ values for H_2F^+ and H_2Cl^+, as shown in Figure 6, where the error bars correspond to the range of several measurements at a constant value of current. As is known in a glow discharge (Teii 1986), Figure 6 shows that the electron density is proportional to the discharge current. To determine k_e, we have to obtain the electron density $[e^-]$, so we utilized a method with a single Langmuir probe (von Engel 1983; Teii 1986). When we set a discharge in a mixture of 9.3 Pa F_2/H_2 and 44 Pa H_2 with a DC current of 200 mA at the probe position between two electrodes, the density was obtained to be (2.65–2.85) $\times$ 10^{11} electrons cm^{-3}. In the case of a pure hydrogen discharge (H_3^+ production), a density of (2.55–2.75) $\times$ 10^{11} electrons cm^{-3} was obtained. Since the difference in the density between conditions producing H_3^+ and H_2F^+ was small, we assumed the same density for the production of H_2Cl^+. By averaging three measurements, we obtained $[e^-] = (2.78 \pm 0.56) \times 10^{11}\,cm^{-3}$, where the error corresponds to the range of the observed values.

We also derived the ion density at $t = 0$ for comparison with the electron density, although the value is not necessary for deriving the rate constant in the case of the first-order reaction scheme. The procedure is described by Bernath (2005), and we used the transition moment of 0.322 Debye for the $H_2F^+\nu_3$ band, reported by Bunker et al. (1990). The rotational temperature was fixed at the value of 209 K determined from Fourier-transform absorption spectroscopy of H_3^+ (Fujimori et al. 2013). The partition function was calculated numerically from the lowest energy level, until the new value does not contribute to 1% of the summed total value. The estimated abundance of H_2F^+ is $(3.3 \pm 0.7) \times 10^{10}\,cm^{-3}$, where we confirmed that the ion density is an order of magnitude smaller than the electron density $[e^-]$ in the present experimental condition.

By using the $k_e[e^-]$ value of Figure 6 at 200 mA, we obtained the following dissociative recombination rate constants:

$$k_e(H_2F^+) = (1.08 \pm 0.29) \times 10^{-7}\,cm^3\,s^{-1}$$
$$k_e(H_2Cl^+) = (0.46 \pm 0.05) \times 10^{-7}\,cm^3\,s^{-1}.$$

The present value for H_2F^+ is in agreement with that obtained by the flowing afterglow experiment, and eight times smaller than the value calculated from Equations (1) and (2) at 209 K. It is noted that in interstellar space the ion is distributed in only the lowest rotational levels of the ortho and para states. On the other

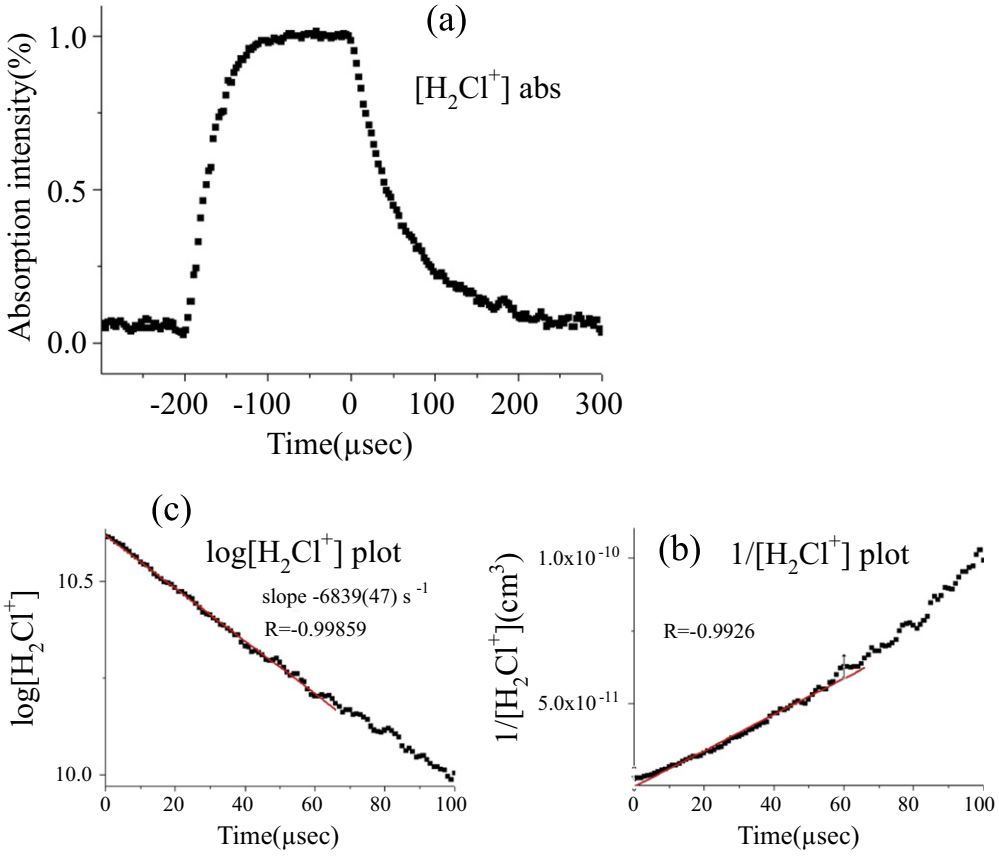

Figure 5. (a) Time-resolved spectrum of the $H_2Cl^+\nu_3$ band, $J_{KaKc} = 6_{06} \leftarrow 5_{05}$ and $6_{16} \leftarrow 5_{15}$ transitions at 2691.24 cm^{-1} obtained by a pulsed discharge with peak current of 300 mA, (b) $1/N$ fit, (c) exponential fit.

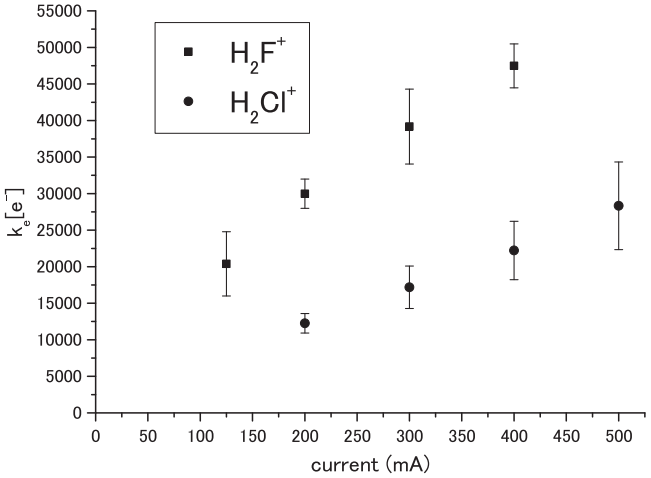

Figure 6. Product of the dissociative recombination constant (k_e) and electron density [e^-] obtained by the fittings of decay curves at various values of discharge current.

hand, the present laboratory measurement for H_2F^+ was carried out for the transition from the seventh lowest energy level of ortho, because of weak intensities of transitions from the lowest 1_{01} level. In the case of H_3^+ and HCO^+, the k_e values for several rotaional states are in agreement within the measurement error limit (Amano 1990). So we assume the same rate for the laboratory and the astronomically observed levels. The k_e value of H_2Cl^+ is half of that given by Equation (3), and a factor 2 larger than that of HCl^+ at 209 K (Novotny et al. 2013).

5. DISCUSSION

The k_e value of H_2F^+ has been determined experimentally at 209 K. The present method is not applicable for lower temperatures, because of the adhesion of the reactants on the glass surface. In interstellar diffuse clouds, the translational temperature is expected to be around 50 K, so we estimated the k_e value by using temperature-dependent terms of Equations (1)–(3) and the present values for the magnitude terms, and found $k_e(50\,K) = 2.2(5) \times 10^{-7}$ and $1.6(4) \times 10^{-7}\,cm^3\,s^{-1}$ for H_2F^+ and H_2Cl^+, respectively. The difference in dissociative recombination rates between H_2F^+ and H_2Cl^+ is not large. Since the temperature-dependent terms of Equations (1)–(3) have not been confirmed experimentally, there may be ambiguity in the estimation. However, even with the same temperature dependence for both rates, the difference is only a factor of 2.3. Therefore, the observed small interstellar abundance of H_2F^+ compared with that of H_2Cl^+ is thought to be mainly due to the production mechanism.

The present value of $k_e(50\,K)$ for H_2Cl^+ is 3.4 times smaller than that derived from Equation (3). This smaller rate increases the abundance of H_2Cl^+ and is in better agreement with astronomical observations, where the observed H_2Cl^+ ion is reported to be 5–10 times (Neufeld et al. 2012, 2015) more abundant than the estimate in previous chemical models of diffuse clouds.

The ionization potentials of Cl and HCl are smaller than that of hydrogen. On the other hand, F and HF have larger ionization energies than hydrogen. The H_2Cl^+ ion is thought to

be produced via two routes in interstellar space:

$$Cl^+ + H_2 \rightarrow HCl^+ + H \quad (9)$$

$$HCl^+ + H_2 \rightarrow H_2Cl^+ + H \quad (10)$$

$$HCl + H_3^+ \rightarrow H_2Cl^+ + H_2. \quad (11)$$

In diffuse clouds, the presence of HCl^+ is important for production of H_2Cl^+ by a reaction with H_2, and the ion has been detected by *Herschel* HIFI (De Luca et al. 2012). On the other hand, F and HF are not ionized by the interstellar radiation field, although the reaction of F^+ with H_2 produces HF^+. Therefore, a possible route for H_2F^+ production is thought to be

$$HF + H_3^+ \rightarrow H_2F^+ + H_2 \quad (12)$$

with a formation rate $k_f(H_3^+) = 1.2 \times 10^{-8}(T/300\ \mathrm{K})^{-0.15}\ \mathrm{cm^3\ s^{-1}}$ (Neufeld et al. 2005). Recently, the detection of CF^+ toward PKS 1830−211 (SW) has been reported with a column density of $5.5 \times 10^{12}\ \mathrm{cm^{-2}}$ (Muller et al. 2016). If the reaction of HF and C^+ is the main route for the production of CF^+, the CF^+ abundance is given in the steady-state approximation as follows:

$$[CF^+] = \frac{k_f(CF^+)[HF][C^+]}{k_e(CF^+)[e^-]} \quad (13)$$

where $k_f(CF^+)$ denotes the formation rate of CF^+ by the reaction $HF + C^+$, and $k_e(CF^+)$ the dissociative recombination rate for $CF^+ + e$. A similar formula is given for H_2F^+:

$$[H_2F^+] = \frac{k_f(H_2F^+)[HF][H_3^+]}{k_e(H_2F^+)[e^-]}. \quad (14)$$

From Equations (13) and (14) the abundance ratio of H_2F^+ and CF^+ is given as follows:

$$\frac{[H_2F^+]}{[CF^+]} = \frac{k_f(H_2F^+)k_e(CF^+)[H_3^+]}{k_f(CF^+)k_e(H_2F^+)[C^+]} = 1.7\frac{k_e(CF^+)[H_3^+]}{k_e(H_2F^+)[C^+]} = 1.6\frac{[H_3^+]}{[C^+]} \quad (15)$$

where the last part is obtained by using the present $k_e(H_2F^+)$. Gerin et al. (2015) reported an abundance ratio $[C]/[H] = (1.5 \pm 0.4) \times 10^{-4}$ in diffuse clouds by *Herschel* observation of C^+. The $[H_3^+]$ abundance is estimated to be $\zeta[H_2]/k_e(H_3^+)[e^-]$ (McCall et al. 2002), where ζ is the cosmic-ray ionization rate and $k_e(H_3^+)$ the dissociative recombination rate constant. Considering the fraction of protons in H_2 (McCall et al. 2002), when we assume $\zeta = 2 \times 10^{-16}\ \mathrm{s^{-1}}$ (Indriolo et al. 2007), $k_e(H_3^+) = 2 \times 10^{-7}\ \mathrm{cm^3\ s^{-1}}$, and $[e^-] = [C]$, the H_2F^+ abundance is expected to be 3.5% of that of CF^+, that is, $[H_2F^+] = 1.9 \times 10^{11}\ \mathrm{cm^{-2}}$ toward PKS 1830−211, which is smaller than the present upper limit of $8.8 \times 10^{11}\ \mathrm{cm^{-2}}$. Non-detection of H_2F^+ toward W31C, NGC 6334 I, and PKS 1830−211 may be explained by the low abundance of H_3^+. On the other hand, the Galactic center source GC IRS 21 has been reported with a large H_3^+ column density of $61.3 \times 10^{14}\ \mathrm{cm^{-2}}$ (Goto et al. 2008). However, the continuum level in the 760 GHz region is too low to detect absorption lines of the H_2F^+ ion. Only five sources have been observed in the present study, so further searches will be necessary to detect the H_2F^+ion in sources with high H_3^+ abundance and a high continuum level.

6. SUMMARY

The HF molecule was detected in the $z = 0.89$ absorber in front of PKS 1830–211 with ALMA, and its abundance relative to H_2 ($>1.7 \times 10^{-8}$) is similar to that of other diffuse clouds in the Galaxy, indicating that HF is an excellent tracer of molecular hydrogen even in the interstellar medium of distant galaxies. In spite of the abundant HF, the protonated H_2F^+ ion is detected neither toward PKS 1830–211 nor toward a sample of four Galactic sources (W31C, NGC 6334 I, IRS 21, and 2Mass J1747). In contrast, the H_2Cl^+ ion is detected with a column density more than an order of magnitude higher than that of H_2F^+ in the observed sources. Laboratory experiments on dissociative recombination reactions provide a smaller rate for H_2F^+ than the previous prediction.

This paper makes use of the following ALMA data: ADS/JAO.ALMA#2013.1.01099.S. ALMA is a partnership of ESO (representing its member states), NSF (USA), and NINS (Japan), together with NRC (Canada), NSC and ASIAA (Taiwan), and KASI (Republic of Korea), in cooperation with the Republic of Chile. The Joint ALMA Observatory is operated by ESO, AUI/NRAO, and NAOJ.

HIFI has been designed and built by a consortium of institutes and university departments from across Europe, Canada, and the United States under the leadership of SRON Netherlands Institute for Space Research, Groningen, The Netherlands and with major contributions from Germany, France, and the US Consortium members are: Canada: CSA, U. Waterloo; France: CESR, LAB, LERMA, IRAM; Germany: KOSMA, MPIfR, MPS; Ireland, NUI Maynooth; Italy: ASI, IFSI-INAF, Osservatorio Astrofisico di Arcetri-INAF; Netherlands: SRON, TUD; Poland: CAMK, CBK; Spain: Observatorio Astronomico Nacional (IGN), Centro de Astrobiologia (CSIC-INTA). Sweden: Chalmers University of Technology—MC2, RSS & GARD; Onsala Space Observatory; Swedish National Space Board, Stockholm University—Stockholm Observatory; Switzerland: ETH Zurich, FHNW; USA: Caltech, JPL, NHSC.

We thank Mina Imai for her contribution to the initial analysis of *Herschel* HIFI data. The present study was partly supported by the Grant-in-Aid from the Ministry of Education, Culture, Sports, Science and Technology of Japan (grant no. 21104003).

REFERENCES

Adam, N. G., & Smith, D. 1988, CPL, 144, 11
Agúndez, M., Cernicharo, J., Waters, L. B., , F. M., et al. 2011, A&A, 533, L6
Amano, T. 1988, ApJL, 329, L121
Amano, T. 1990, JChPh, 92, 6492
Amano, T., Matsushima, F., Shiraishi, T., et al. 2012, JChPh, 137, 134308
Bernath, P. 2005, Spectra of Atoms and Molecules (New York: Oxford Univ. Press)
Bunker, P. R., Jensen, P., Wright, J. S., & Hamilton, I. P. 1990, JMoSp, 144, 310
Cernicharo, J., & Guélin, M. 1987, A&A, 183, L10
De Luca, M., Gupta, H., Neufeld, D., et al. 2012, ApJ, 751, 37
Emprechtinger, M., Monje, R. R., van der Tak, F. F. S., et al. 2012, ApJ, 756, 136
Faure, A., Hily-Blant, P., Le Gal, R., Rist, C., & Pineau des Forêts, G. 2013, ApJL, 770, L2

Fujimori, R., Hirata, Y., Morino, I., & Kawaguchi, K. 2013, JPhCh, A117, 9882
Fujimori, R., Kawaguchi, K., & Amnao, T. 2011, ApJL, 729, L2
Geppert, W. D., & Larsson, M. 2008, MolPh, 106, 2199
Gerin, M., Ruaud, M., Goicoechea, J. R., et al. 2015, A&A, 573, 30
Godard, B., Falgarone, E., Gerin, M., Hily-Blant, P., & de Luca, M. 2010, A&A, 520, 20
Goto, M., Usuda, T., Geballe, T. R., et al. 2011, PASJ, 63, L13
Goto, M., Usuda, T., Nagata, T., et al. 2008, ApJ, 688, 306
Hovde, D. C., Keim, E. R., & Saykally, R. J. 1989, MolPh, 68, 599
Indriolo, N., Geballe, T. R., Oka, T., & McCall, B. J. 2007, ApJ, 671, 1736
Lee, S. K., Amano, T., Kawaguchi, K., & Oldani, M. 1988, JMoSp, 130, 1
Lis, D. C., Pearson, J. C., Neufeld, D. A., et al. 2010, A&A, 521, L9
Lodders, K., Palme, H., & Gail, H. P. 2009, Landolt-Bornstein, New Series, Astronomy and Astrophysics (Berlin: Springer)
Martí-Vidal, I., Vlemmings, W., Muller, S., & Casey, S. 2014, A&A, 563, 136
McCall, B. J., Hinkle, K. H., Greballe, T. R., et al. 2002, ApJ, 567, 391
McCall, B. J., Huneycutt, A. J., Saykally, R. J., et al. 2004, PhRv, 70, 052716
Monje, R. R., Emprechtinger, M., Phillips, T. G., et al. 2011a, ApJL, 734, L23
Monje, R. R., Lis, D. C., Roueff, E., et al. 2013, ApJ, 767, 81
Monje, R. R., Lord, S., Falgarone, E., et al. 2014, ApJ, 785, 22
Monje, R. R., Phillips, T. G., Peng, R., et al. 2011b, ApJ, 741, 21
Morisawa, Y., Fushitani, M., Kato, Y., et al. 2006, ApJ, 642, 954
Muller, S., Beelen, A., Black, J. H., et al. 2013, A&A, 551, 109
Muller, S., Beelen, A., Guélin, M., et al. 2011, A&A, 535, 103
Muller, S., Black, J. H., Guelin, M., et al. 2014a, A&A, 566, 6
Muller, S., Combes, F., Guélin, M., et al. 2014b, A&A, 566, 112
Muller, S., & Guélin, M. 2008, A&A, 491, 739
Muller, S., Kawaguchi, K., Black, J. H., & Amano, T. 2016, A&A, 566, L5
Neufeld, D. A., Black, J. H., Gerin, M., et al. 2015, ApJ, 807, 54
Neufeld, D. A., Roueff, E., Snell, R., et al. 2012, ApJ, 748, 37
Neufeld, D. A., Schilke, P., Menten, K. M., et al. 2006, A&A, 454, L37
Neufeld, D. A., Sonnentrucker, P., Phillips, T. G., et al. 2010, A&A, 518, L108
Neufeld, D. A., & Wolfire, M. G. 2009, ApJ, 706, 1594
Neufeld, D. A., Wolfire, M. G., & Schilke, P. 2005, ApJ, 628, 260
Neufeld, D. A., Zmuidzinas, J., Schilke, P., & Phillips, T. G. 1997, ApJL, 488, L141
Novotny, O., Becker, A., Buhr, H., et al. 2013, ApJ, 777, 54
Okabayashi, Y., Miyamoto, Y., Tang, J., & Kawaguchi, K. 2015, CPL, 619, 144
Ossenkopf, V., Müller, H. S. P., Lis, D. C., et al. 2010, A&A, 518, L111
Phillips, T. G., Bergin, E. A., Lis, D. C., et al. 2010, A&A, 518, L109
Plašil, R., Glosik, J., Poterya, V., et al. 2002, IJMSp, 218, 105
Rangwala, N., Maloney, P. R., Glenn, J., et al. 2011, ApJ, 743, 94
Schilke, P., Neufeld, D. A., Müller, H. S. P., et al. 2014, A&A, 566, A29
Sonnentrucker, P., Neufeld, D. A., Phillips, T. G., et al. 2010, A&A, 521, L12
Sonnentrucker, P., Wolfire, M., Neufeld, D. A., et al. 2015, A&A, 806, 49
Takakuwa, S., Kawaguchi, K., Mikami, H., & Saito, M. 2001, PASJ, 53, 251
Teii, S. 1986, Purazuma Kisokougaku (Tokyo: Uchida Rokakuho) (in Japanese)
van der Werf, P. P., Isaak, K. G., Meijeerink, R., et al. 2010, A&A, 518, L42
von Engel, A. 1983, Electric Plasmas: Their Nature and Uses (New York: Taylor and Francis)
Zernickel, A., Schilke, P., Schmiedeke, A., et al. 2012, A&A, 546, A87